

Analysis of Contact Width and Contact Stress of Three-Layer Corrugated Metal Gasket

I. Made Gatot Karohika, Shigeyuki Haruyama, Ken Kaminishi, Oke Oktavianty, Didik Nurhadiyanto

Abstract—Contact width and contact stress are important parameters related to the leakage behavior of corrugated metal gasket. In this study, contact width and contact stress of three-layer corrugated metal gasket are investigated due to the modulus of elasticity and thickness of surface layer for 2 type gasket (0-MPa and 400-MPa mode). A finite element method was employed to develop simulation solution to analysis the effect of each parameter. The result indicated that lowering the modulus of elasticity ratio of surface layer will result in better contact width but the average contact stresses are smaller. When the modulus of elasticity ratio is held constant with thickness ratio increase, its contact width has an increscent trend otherwise the average contact stress has decreased trend.

Keywords—Contact width, contact stress, layer, metal gasket, corrugated, simulation.

I. INTRODUCTION

A gasket is an important device in the piping industry that is used to create a static seal under various conditions of the mechanical assembly. Since asbestos gasket was banned in Japan, the research of a new material as the asbestos substitution is developed. One of the materials that have a good perspective as asbestos gasket substitution is metal gasket because of its effectiveness in high-temperature and high-pressure environment. A super seal metal gasket was proposed by Saeed et al. [1]; a new 25 A metal gasket with corrugated shape was optimized to leakage performance using contact area as an evaluation creation on design. Haruyama et al. [2] continue the research of 25 A size metal gasket design parameter to investigate the limit size of contact width.

Choiron et al. [3] used pressure sensitive paper to get a validation of contact width measurement. The result indicated the similar trend data between experiment and simulation. Researches [1]-[3] optimize metal gasket without considering forming effect. Nurhadiyanto et al. [4] optimized the gasket based on an elastic contact stress (0-MPa mode) and plastic contact stress (400-MPa mode) considering forming effect. The helium leakage test shows that the gasket in 400-MPa mode has better sealing performance than the gasket in 0-MPa mode. The Helium leak test based on JIS Z2330 and JIS J2331 standards

showed that gasket 0-MPa mode was not leaked on the 100 KN axial force while the gasket 400-MPa mode was not leaked on 80 KN axial force. The leakage behavior of metal gasket also depends on surface roughness used. Haruyama et al. [5] developed a gasket model that includes the flange surface roughness effect. The research investigated contact width, contact stress, and force per unit length of the gasket in contact with a flange having different surface roughness obtained by simulation, and the leakage performance obtained through a helium leakage test. The simulation and experiment showed the same result that gasket in 400-MPa mode better than gasket in 0-MPa mode. Haruyama et al. [6] studied the real measurement result of contact width before and after use based on flange's surface roughness effect. The result indicated that the real contact width for the flange with smoother surface roughness is wider than the rougher one. Nurhadiyanto et al. [7] studied the real contact stress and contact width when leakage started on 25A-size metal gasket through simulation and experiment for gasket 400-MPa mode. A comparison of the simulation result and experiment data showed good agreement. The result justified that the leakage did not occur on the real contact width 0.195 mm and average contact stress 800MPa for the gasket contact with a flange having surface roughness 3.5 μ m.

Study for the corrugated metal gasket is still underway to improve its performance. In [5], it is also mentioned that the performance of gasket decreases with increasing the surface roughness of the flange. The utilization of material softer than the base material as a surface covering material is already widely used to improve performance gaskets. Al, Cu, and Ni as the cover layer have also been used on the elastic metal gasket O-ring named "Helicoflex" [8], [9]. Haruyama et al. [10] developed three-layer corrugated metal gasket with SUS304 as base metal and aluminum, copper, nickel as the surface layer. The surface layer thickness used was 0.1 mm for upper and lower layer respectively [4]. A finite element method is employed to determine the effect of a different material layer and tangent modulus material layer on contact width and contact stress of three-layer corrugated metal gasket. However, in [10], there is no discussion about the effect of modulus elasticity ratio for more materials and effect of surface layer thickness. In this study, we investigated the effect of modulus elasticity ratio and thickness ratio on contact width and contact stress using Finite Element Analysis (FEA). The modulus elasticity ratio is the ratio of surface layer modulus elasticity to SUS304. Thickness ratio is the ratio of base material thickness to total thickness gasket. The result will give us the mapping of the effects of the layer material selection and thickness on contact width and contact stress. The distribution maps of the

M.G. Karohika and O. Oktavianty, S. Haruyama, K. Kaminishi are with Yamaguchi University, Japan (e-mail: u503wc@yamaguchi-u.ac.jp, u504wc@yamaguchi-u.ac.jp, kaminishi@yamaguchi-u.ac.jp, haruyama@yamaguchi-u.ac.jp).

D. Nurhadiyanto is with Yogyakarta State University (email: didiknur@uny.ac.id)

three-layer metal gasket plotted in this study are very important in the design process of the three-layer metal gasket and could function as a key reference in the future.

II. MATERIALS AND METHODS

Fig. 1 shows a corrugated metal gasket which is to be inserted between flanges and dimension of a three-layer corrugated metal gasket. Gaskets consist of two types: 0-MPa mode and 400-MPa mode, the detailed dimension of this gasket are described in Table I. Three layers of sheet metal assumed to be fully bound; consequently, delamination interface is beyond the scope of this paper.

In this study, a gasket is divided into two processes by using forming and tightening simulation as shown in Fig. 2. A gasket was modeled and then the deformation mode was investigated using finite element method analysis software MSC. Marc. First, using two-dimensional assumptions, an axis-symmetric model was adopted for the forming process simulation in the axial direction between the upper and lower dies. Second, the gasket shape is produced then compressed in the axial direction between the upper and lower flanges to simulate the relationship between the axial force, average contact stress, and contact width. Both the upper and lower dies and flanges are assumed to be rigid bodies. Flowchart of the stage simulation gasket by considering the type of gasket, thickness ratio and modulus of elasticity ratio effects is shown in Fig. 3.

Based on [11], the stiffness to weight ratio of a laminate is one of its most attractive properties when considering a need for weight reduction. The stiffness of a laminated sheet is defined as the resistance to elastic deformation in bending, which is equivalent to the bending modulus of the material. The elastic modulus of a homogeneous sheet is generally the same in tension and in bending, whereas the bending modulus varies with the volume fraction of the base. When the properties of the laminate are symmetrical about its neutral axis, then the tensile and bending moduli of elasticity, E_T , and E_B can be expressed using the rule of mixtures and simple bending theory from which the specific stiffness can be estimated from known density of face metal and the base:

$$E_T = E_s V_s + E_b(1 - V_s) \quad (1)$$

$$V_s = A_s t_s / A_{Total} t_{Total} \quad (2)$$

If $A_s = A_{Total}$, then;

$$V_s = t_s / t_{Total} \quad (3)$$

$$E_B = E_s [1 - (1 - V_s)^3] + E_b(1 - V_s)^3 \quad (4)$$

where E and V are Young's modulus and volume fraction, respectively, of an individual component, and subscripts s and b refer to the surface metal and the base materials, respectively.

The thickness gasket total (T_g) for gasket 0-MPa mode is 1.2 mm and 1.5 mm for gasket 400-MPa mode. The overall length (L) of the gasket is 19.5 mm (Fig. 1). Characteristics of the base material (SUS304) are shown Table II. For 0-MPa mode, the thickness ratio (T_b/T_g) varies as 1/1.2, 0.8/1.2, 0.6/1.2, 0.4/1.2 and for 400-MPa mode varies as 1.3/1.5, 1.1/1.5, 0.9/1.5, 0.7/1.5, 0.5/1.5. The total thickness of gasket (T_g) is held constant. The modulus of elasticity ratio between the surface layer to the base material (E_s/E_b) varies from 0.08 up to 0.9. The surface layer was considered as an elastic-perfectly-plastic material with σ_{ys}/E_s of 0.001 and work hardening coefficient ratio with E_T/E_s of 0.01. The Poisson's ratio for all surface layer material was 0.3.

TABLE I
OPTIMUM DESIGN OF GASKET 0-MPa AND 400-MPa MODE

No	Design Parameter	0-MPa	400-MPa																							
A	Over Hang (OH)[mm]	3	3																							
B	Pitch 1 (p1) [mm]	4.5	3.5																							
C	Pitch 2 (p2) [mm]	4.5	4.5																							
D	Pitch 3 (p3) [mm]	4.5 <table border="1" style="display: none;" <thead> <tr> <th>No</th> <th>Design Parameter</th> <th>0-MPa</th> <th>400-MPa</th> </tr> </thead> <tbody> <tr> <td>E</td> <td>Lip Height (h)[mm]</td> <td>0.35</td> <td>0.3</td> </tr> <tr> <td></td> <td>Lip Height (h1)[mm]</td> <td>0.39</td> <td>0.33</td> </tr> <tr> <td>F</td> <td>Convex Radius (R)[mm]</td> <td>3.5</td> <td>2.5</td> </tr> <tr> <td></td> <td>Convex Radius (R1)[mm]</td> <td>3.2</td> <td>2.3</td> </tr> <tr> <td>G</td> <td>Thickness gasket total (Tg)[mm]</td> <td>1.2</td> <td>1.5</td> </tr> </tbody>	No	Design Parameter	0-MPa	400-MPa	E	Lip Height (h)[mm]	0.35	0.3		Lip Height (h1)[mm]	0.39	0.33	F	Convex Radius (R)[mm]	3.5	2.5		Convex Radius (R1)[mm]	3.2	2.3	G	Thickness gasket total (Tg)[mm]	1.2	1.5
No	Design Parameter	0-MPa	400-MPa																							
E	Lip Height (h)[mm]	0.35	0.3																							
	Lip Height (h1)[mm]	0.39	0.33																							
F	Convex Radius (R)[mm]	3.5	2.5																							
	Convex Radius (R1)[mm]	3.2	2.3																							
G	Thickness gasket total (Tg)[mm]	1.2	1.5																							

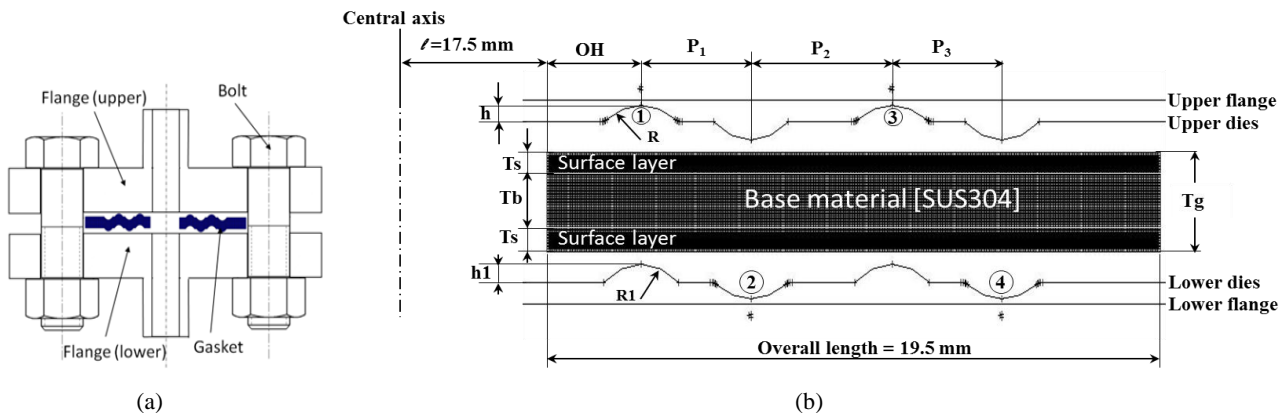
 3.5 || E | Lip Height (h)[mm] | 0.35 | 0.3 |
	Lip Height (h1)[mm]	0.39	0.33
F	Convex Radius (R)[mm]	3.5	2.5
	Convex Radius (R1)[mm]	3.2	2.3
G	Thickness gasket total (Tg)[mm]	1.2	1.5


Fig. 1 (a) Schematic section of gasket-flange (b) dimension of three-layer gasket

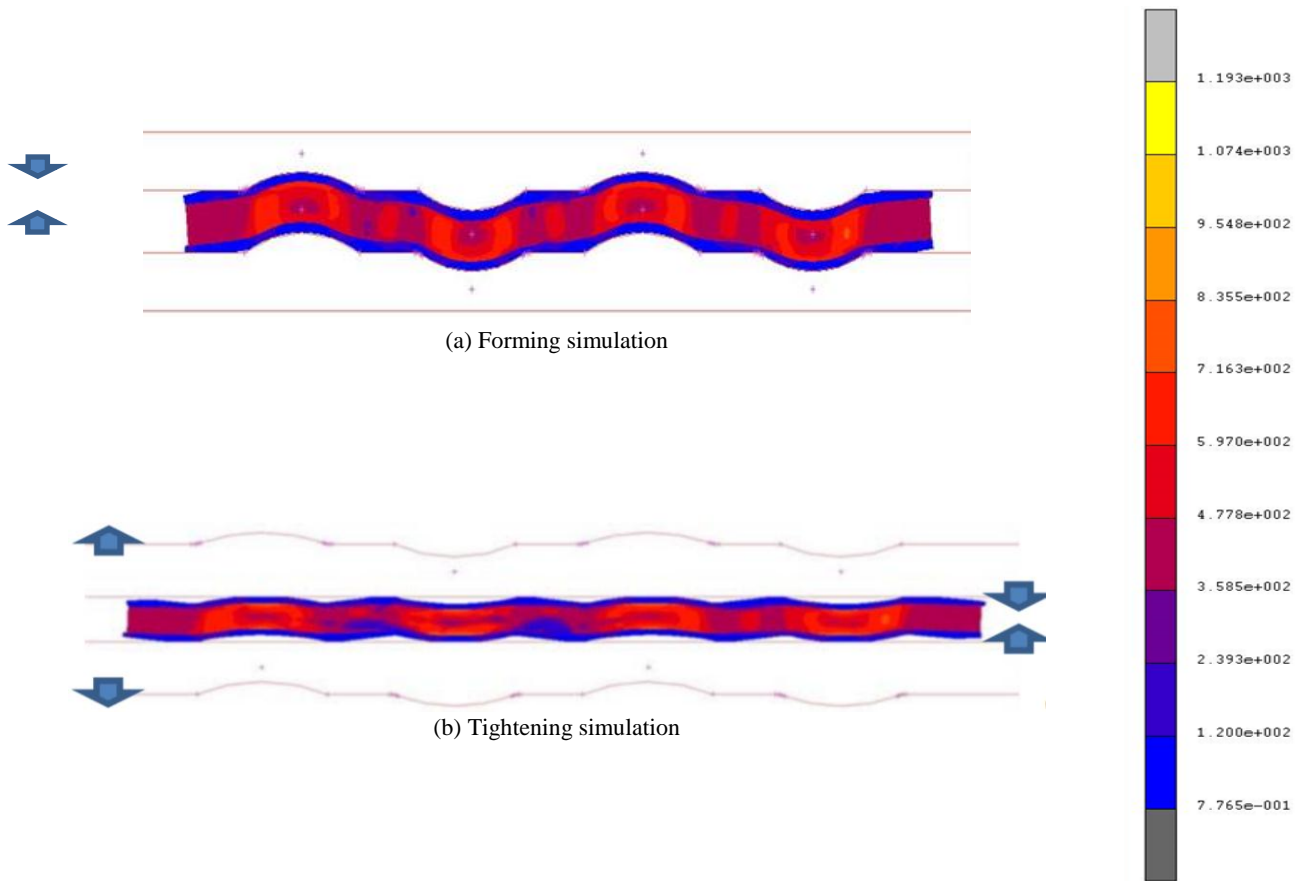


Fig. 2 Axisymmetric model three-layer gasket (a) Forming process (b) Tightening process

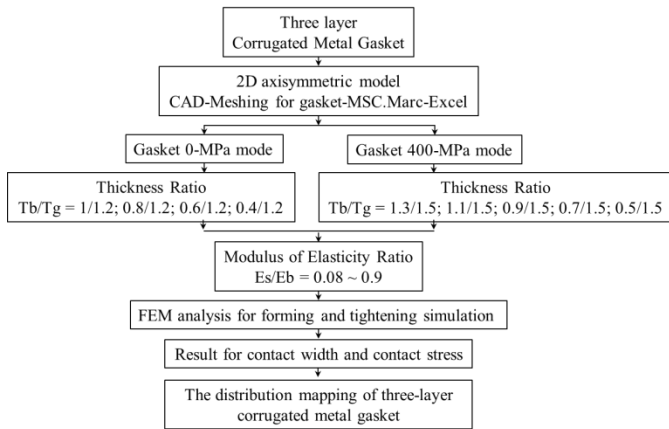


Fig. 3 Flowchart the stage of the three layer gasket simulation

III. RESULT AND DISCUSSION

The contact stress and contact width evaluation were performed only for the convex portion of the gasket, which is effective at reducing the leakage.

1. Effect of Modulus of Elasticity Ratio on Contact Width and Contact Stress

Firstly we plot graphic with vertical axis giving the aspect ratio of modulus of elasticity of the surface layer material to SUS304 while contact width or average contact stress is given along the horizontal axis. To describe the effect of modulus of

elasticity ratio on contact width and average contact stress we use thickness ratio (T_b/T_g) 1/1.2 as an example.

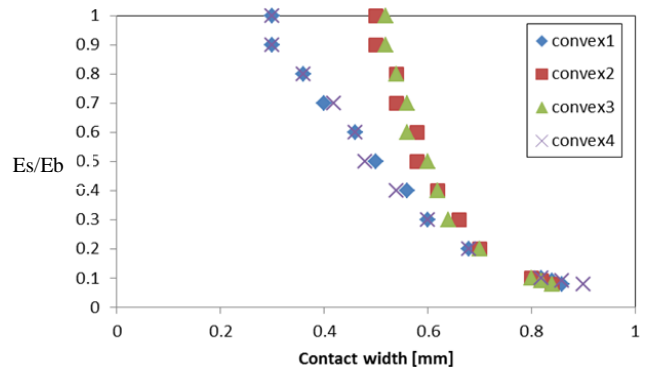


Fig. 4 The mapping contact width vs. E_s/E_b for three-layer corrugated metal gasket (0-MPa mode, $T_b/T_g=1/1.2$, 100kN)

TABLE II
PROPERTIES OF SUS304 USED IN SIMULATION

Material	Nominal Stress (σ) [MPa]	Tangent Modulus [MPa]	Modulus of Elasticity (E) [GPa]	Poisson ratio (ν)
SUS304	398.83	1900.53	210	0.3

Fig. 4 shows a distribution map of the contact width with the modulus of elasticity ratio from 0.08 up to 1 for gasket 0-MPa mode, $T_s = 0.1$ mm, on 100 kN axial force. We choose axial force 100 kN because on this axial force gasket 0-MPa single layer SUS304, not leakage based on helium leak rate test [5].

Value $E_s/E_b = 1$ indicated gasket single layer SUS304. From Fig. 3 for E_s/E_b value we got convex 2 and 3 have the higher contact width than convex 1 and 4, therefore the analysis focus only on convex 2 and 3.

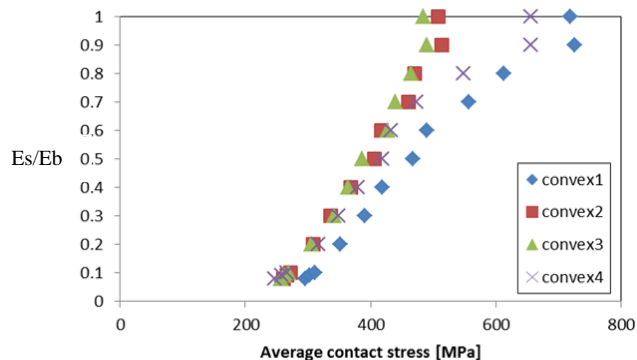


Fig. 5 The mapping average contact stress vs. E_s/E_b for three-layer corrugated metal gasket (0-MPa mode, $T_b/T_g=1/1.2$, 100kN)

Fig. 5 shows a distribution map of the average contact stress with the modulus of elasticity ratio from 1 down to 0.08 for gasket 0-MPa mode, $T_s = 0.1$ mm, on 100 KN axial force. It shows if value E_s/E_b decrease, the average contact stress value decrease for each convex.

Fig. 6 shows the deformation shape for single layer SUS304, gasket single layer SUS304, the 0-MPa mode at the axial force 100 KN. For gasket single layer at 100 KN there is a small contact between inside and outside flat portion gasket with flange, so when gasket tightens, the convex 1 and 4 tend to move to inner and outer radius of gasket, so the deformation concentration focuses on convex 2 and 3, therefore contact width on convex 2 and 3 is higher than convex 1 and 4. On the other hand, contact width convex 1 and 4 is higher than convex 2 and 3. Fig. 7 shows there is big contact between inside and outside flat portion gasket with flange when gasket tightens, so convex 1 and 4 tend not to move to the inner and outer radius of

gasket and more focus to deformation, therefore contact width on convex 1 and 4 increase significantly.

Fig. 8 shows the percentage contact width changes due to the modulus elasticity ratio. The values of E_s/E_b decrease until 0.1 show significant contact width increase after that tend to constant. Otherwise, Fig. 9 shows the average contact stress decrease significantly until E_s/E_b 0.1, after that the decrease not significant. The minus sign indicates average contact stress decrease. If we compare Figs. 8 and 9, the percentage increase in contact width is higher than the percentage decrease in average contact stress.

Fig. 10 shows a distribution map of the contact width with the modulus of elasticity ratio from 0.09 up to 1 for gasket 400-MPa mode, $T_s = 0.1$ mm, on 100 KN axial force. Value 1 indicated gasket single layer SUS304. From Fig. 9 for E_s/E_b value we got convex 2 and 3 have the higher contact width than convex 1 and 4. When E_s/E_b value less than 1, it seemed there is different behavior for each convex. Here shows for convex 2 and 3 there is no significant change until E_s/E_b 0.2. For convex 1 also shown there is no change until E_s/E_b 0.4 after that contact width increase significant. For convex 3, when E_s/E_b decreases, contact width look increases.

Fig. 11 shows a distribution map of the average contact stress with the modulus of elasticity ratio from 0.09 up to 1 for gasket 400-MPa mode, $T_s = 0.1$ mm, on 100 KN axial force. The figure shows lower modulus of elasticity ratio, the average contact stress decreases for each convex.

The inconsistency trend for this 400-MPa mode happens because the deformation shape when forming process as shown in Figs. 3 and 12. Fig. 12 shows a gasket defect occurred on the radius shape of convex contact when forming process, and there is a dent at the peak of convex. Fig. 13 also shows a gasket defect occurred on the radius shape of convex contact when forming process.

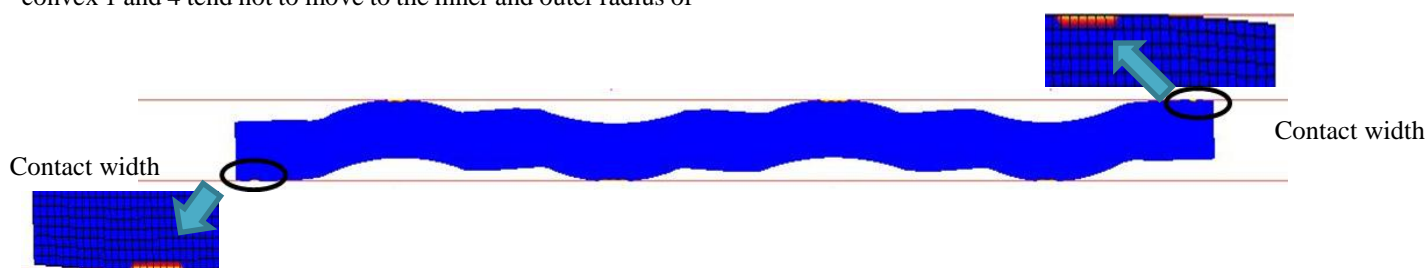


Fig. 6 The deformation shape for single layer SUS304, 0-MPa mode, 100 KN axial force

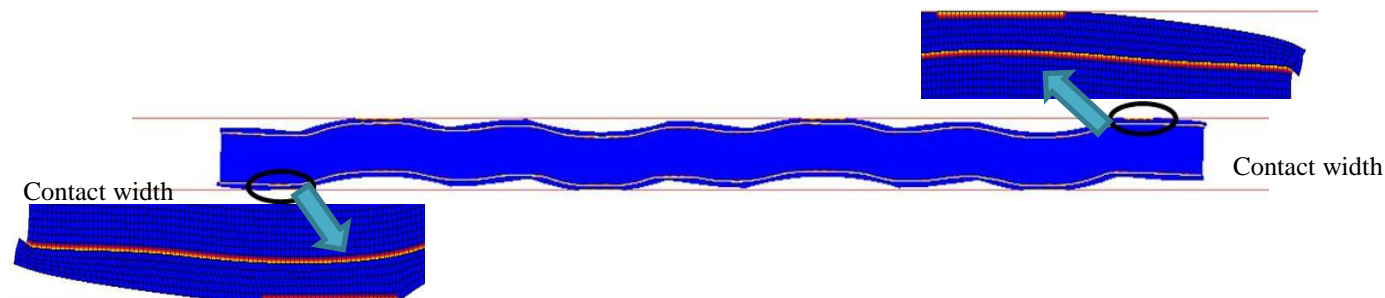


Fig. 7 The deformation shape for three-layer metal gasket 0-MPa, $E_s/E_b = 0.1$, 100 KN axial force

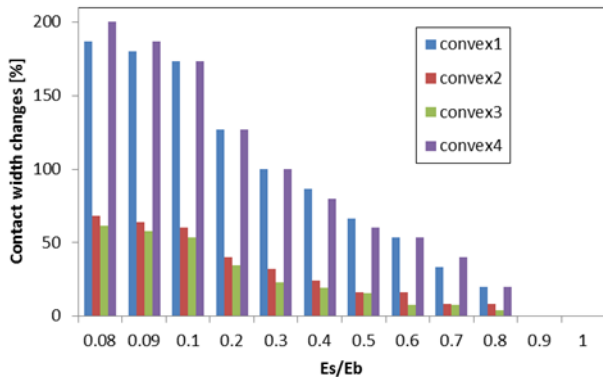


Fig. 8 Percentage contact width, gasket 0-MPa mode, axial force 100 KN

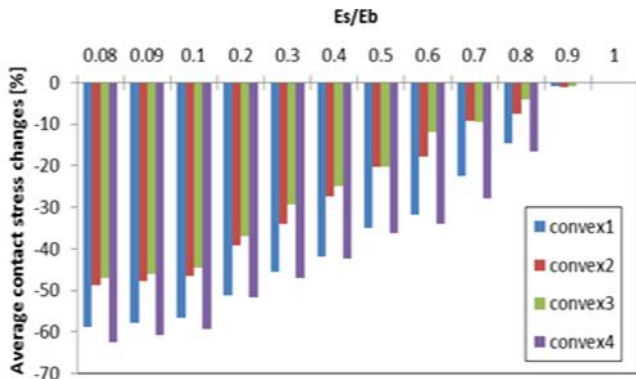


Fig. 9 Percentage average contact stress, gasket 0-MPa mode, axial force 100KN

The contact width change due to the influence modulus of elasticity ratio is shown in Fig. 14. If the values of E_s/E_b decrease, the percentage contact width changes will increase.

The average contact stress change due to the influence modulus of elasticity ratio is shown in Fig. 15. The minus sign indicated average contact stress decrease. For E_s/E_b value 0.9 there is a small decrease of average contact stress although the contact width on the convex section is the same with the single layer. This is because at that time there is a small contact on the flat portion of the gasket, so overall there has been an increase

in the contact width, therefore the average contact stress decrease.

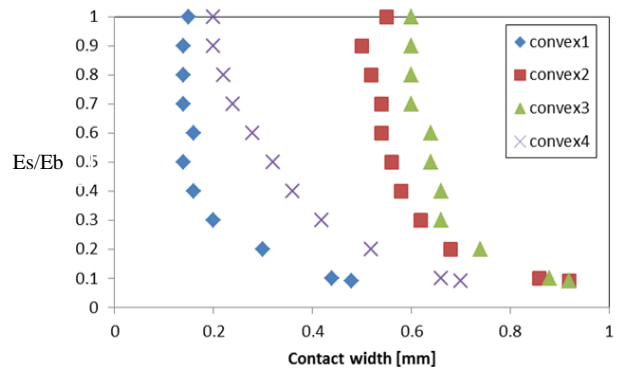


Fig. 10 The mapping contact width - modulus of elasticity ratio for three-layer corrugated metal gasket (400-MPa mode, $T_b/T_g=1/1.5$, 100 KN)

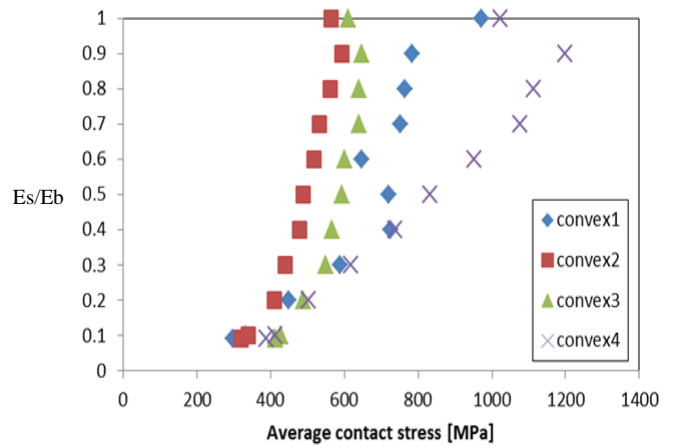


Fig. 11 The mapping average contact stress - modulus of elasticity ratio for three-layer corrugated metal gasket (400-MPa mode, $T_b/T_g=1/1.5$, 100 KN)

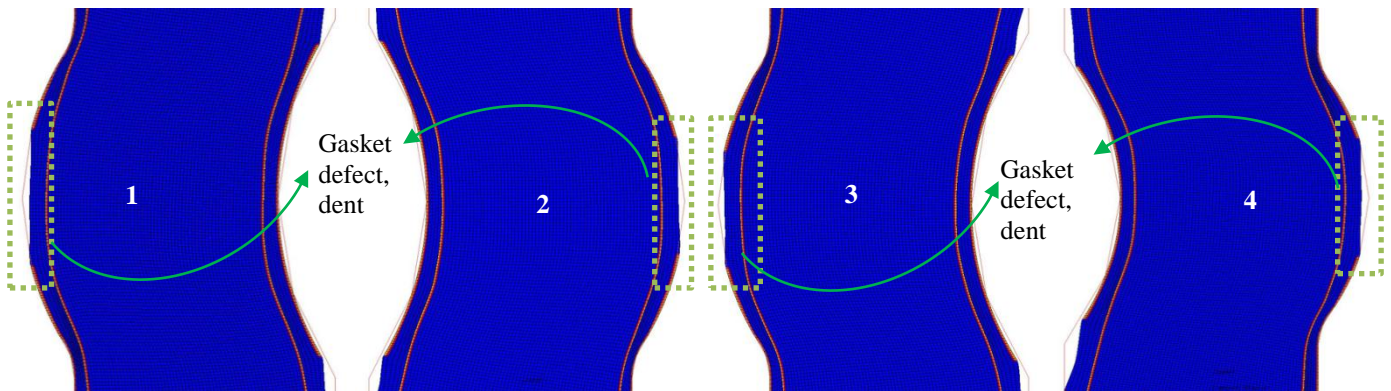


Fig.12 The deformation shape for three-layer metal gasket 400-MPa, $E_s/E_b = 0.1$, forming process.

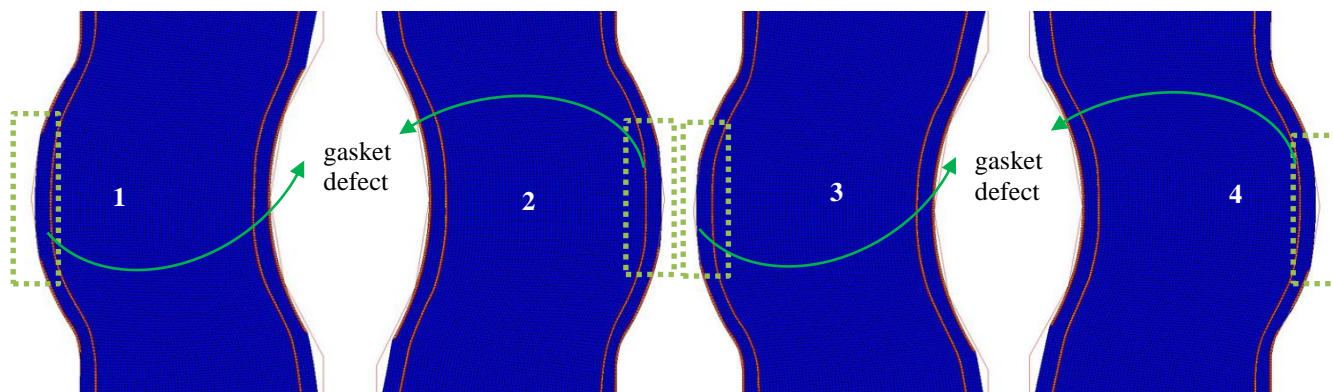


Fig. 13 The deformation shape for three-layer metal gasket 400-MPa, $E_s/E_b = 0.5$, forming process.

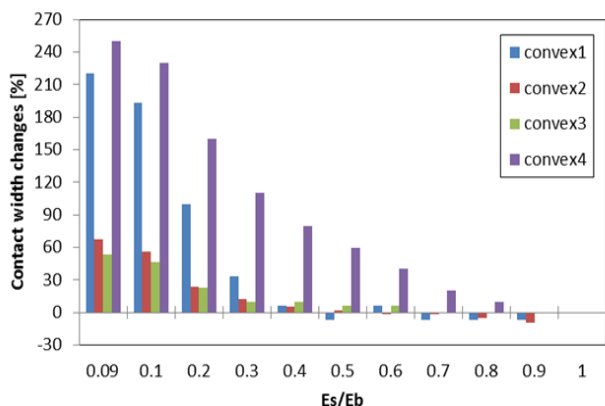


Fig. 14 Percentage contact width increase, gasket 400-MPa mode, axial force 100KN

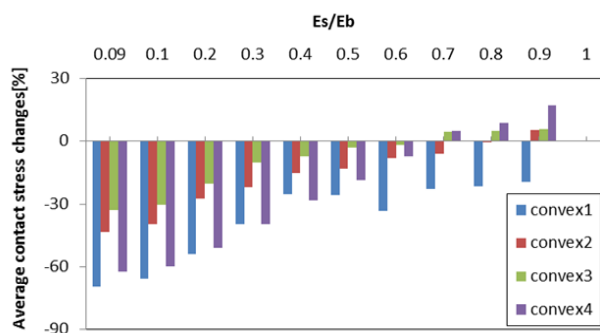


Fig.15 Percentage average contact stress, gasket 400-MPa mode, axial force 100KN

2. Effect of Thickness of the Surface Layer on Contact Width and Contact Stress

To describe the effect of surface layer's thickness on contact width and average contact stress we use the modulus of elasticity ratio 0.1 as an example.

Fig. 16 shows the contact width versus surface layer's thickness for 0-MPa mode gasket, axial force 100KN. The model three-layer show higher contact width compared with single layer SUS304. In gasket SUS304 convex 2 and 3 have higher contact width than convex 1 and 4. For T_b/T_g 1/1.2 until 0.6/1.2 shows with increasing thickness then contact width increases significantly. For 0.4/1.2 there is no significant effect.

Fig. 17 shows the average contact stress versus surface layer's thickness for 0-MPa mode gasket, axial force 100KN. This figure shows the increase in surface layer's thickness will cause a decrease in average contact stress.

Because of the sealing performance of gasket in correlation with contact width, therefore T_b/T_g value 1/1.2, 0.8/1.2 and 0.6/1.2 recommend. For T_b/T_g is 0.4/1.2 not recommended because contact width increase not significant but average contact stress decrease.

The percentage of the contact width changes due to the influence of thickness ratio is shown in Fig. 18. If the thickness of surface layer increase, the percentage of contact width changes will increase.

Otherwise, the average contact stress change due to the thickness ratio effect is shown in Fig. 19. The minus sign indicated average contact stress decrease. This is because at that time there is a small contact on the flat portion of the gasket as shown in Table III, so overall there has been an increase in the contact width, therefore the average contact stress decrease. If comparing Figs. 18 and 19, the percentage increase in contact width is higher than the percentage decrease in average contact stress.

Table III shows the contacts that occur in each flat part of the gasket on the axial force 100KN. Here indicated by the increase in the thickness of the surface causing more flat parts in contact with the flanges. Therefore, the average contact stress on the convex section will decrease.

Fig. 20 shows the contact width versus surface layer's thickness for 400-MPa mode gasket, axial force 100KN. All model three-layer show higher contact width compared with single layer SUS304. In gasket SUS304 convex 2 and 3 have higher contact width than convex 1 and 4. For T_b/T_g 1.3/1.5 until 0.9/1.5 shows with increasing thickness then contact width increases significantly. For 0.7/1.5 and 0.5/1.5 there is no significant effect on contact width.

Fig. 21 shows the average contact stress versus surface layer's thickness for 400-MPa mode gasket, axial force 100KN. This figure shows the increase in surface layer's thickness will cause a decrease in average contact stress.

Because of the sealing performance of gasket in correlation with contact width, therefore Tb/Tg value 1.3/1.5, 1.1/1.5 and 0.9/1.5 recommended. For Tb/Tg 0.7/1.5 and 0.5/1.5 not recommended because contact width increase not significant but average contact stress decrease.

Fig. 22 shows the contact width versus surface layer's thickness for gasket 400-MPa mode, axial force 100KN. All model three- layer show higher contact width compared with single layer SUS304. It shows from Tb/Tg 1.3/1.5 until 0.9/1.5 for convex 2 and 3, there are small contact width increases.

Fig. 23 shows the average contact stress versus surface layer's thickness for 400-MPa mode gasket, axial force 100KN. This figure shows the increase in surface layer's thickness will cause a decrease in average contact stress. If comparing Figs. 22 and 23, the percentage increase in contact width is higher than the percentage decrease in average contact stress.

Table IV shows the forming process simulation for gasket three-layer 400-MPa mode. Here indicated there is the gasket defect and the convex peak dent on forming simulation. The defect decreased by the increase in the thickness of the surface layer. Therefore, the contact width and average contact stress on each convex section result shows not consistency trend.

IV. CONCLUSION

This paper investigated the surface layer material and thickness of surface layer affecting the contact width and

contact stress of the three-layer corrugated metal gasket. The surface layer material needs to be carefully selected to get proper sealing of the flange gasket assembly. Based on FEM analysis the following results were obtained.

1. The modulus of elasticity ratio decreased generates increased contact width but instead contact stress decreases. This result shows the same trend for gasket 0-MPa mode and 400-MPa mode.
2. The thickness ratio gives different contact width and average contact stress result. If the modulus of elasticity ratio is held constant, decrease thickness ratio produces increase contact width but the average contact stress has decreased.
3. The inconsistency trend for gasket three-layer 0-MPa because with decrease E_s/E_b there is increase contact on the flat portion. For 400-MPa the inconsistency trend because the lack of die fill defect on forming process.
4. Based on the simulation, for 0-MPa it is recommended Tb/Tg 1/1.2, and for 400-MPa mode its recommended Tb/Tg 0.9/1.5, 1.1/1.5 and 1.3/1.5 have better sealing performance.
5. The finite element analysis predictions provide a helpful reference for design of three-layer corrugated metal gasket, but experimentation to verify them is recommended.

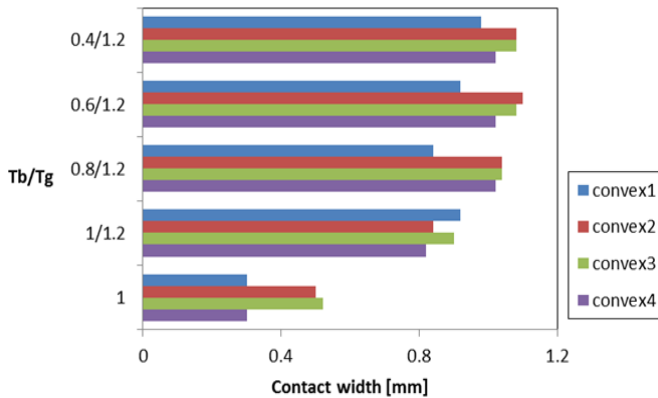


Fig. 16 The contact width vs. Tb/Tg for three-layer corrugated metal gasket (0-MPa mode, $E_s/E_b=0.1$, 100KN)

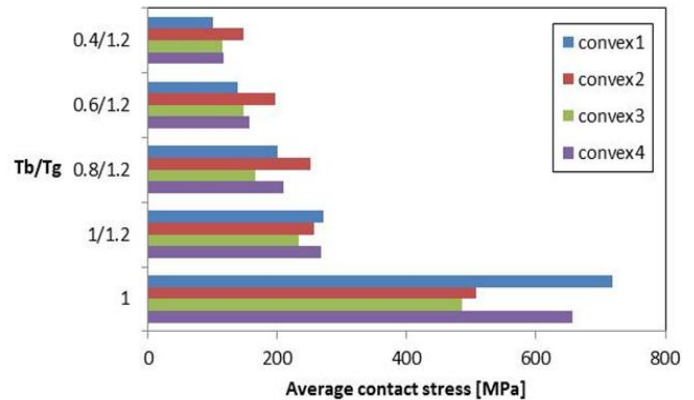


Fig. 17 The average contact stress vs. Tb/Tg for three-layer corrugated metal gasket (0-MPa mode, $E_s/E_b=0.1$, 100KN)

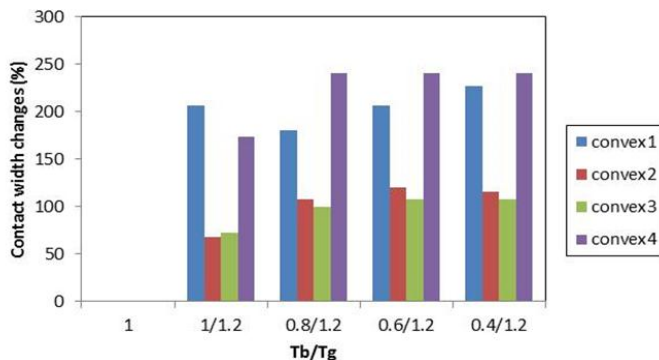


Fig. 18 Percentage contact width increase, gasket 0-MPa mode, axial force 100KN

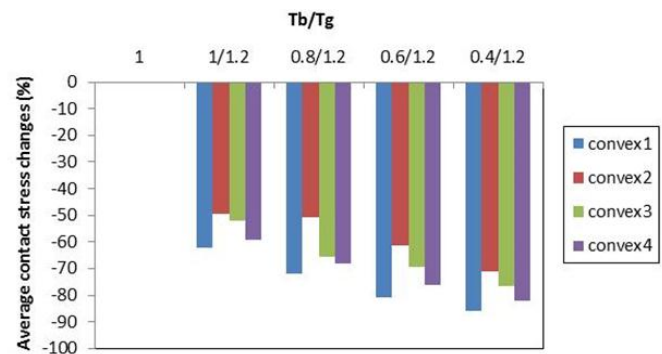


Fig. 19 Percentage average contact stress, gasket 0-MPa mode, axial force 100KN

TABLE III
 CONTACT WIDTH STATUS ON FLAT PORTION GASKET THREE-LAYER 0-MPA MODE, 100kN

Tb/Tg	Inner	Flat 1-2	Flat 2-3	Flat 3-4	Outer
1/1.2		No contact	No contact	No contact	
0.8/1.2				No contact	
0.6/1.2					
0.4/1.2					

Note: Inner means the flat part at the inside radius of the gasket, outer means the flat part at the outside radius of the gasket, flat 1-2 means the flat part between convex1 and convex2, flat 2-3 means the flat part between convex2 and convex3, flat 3-4 means the flat part between convex3 and convex4

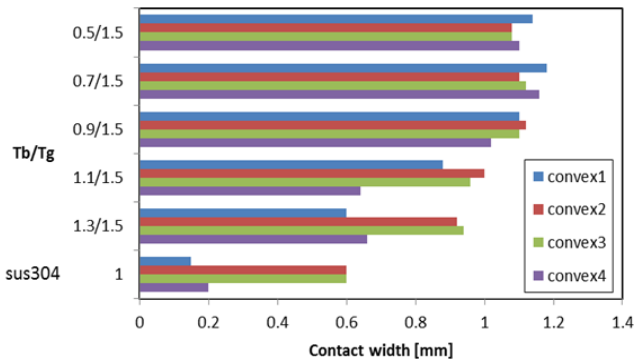


Fig. 20 The contact width vs. Tb/Tg for three-layer corrugated metal gasket (400-MPa mode, $E_s/E_b=0.1$, 100kN)

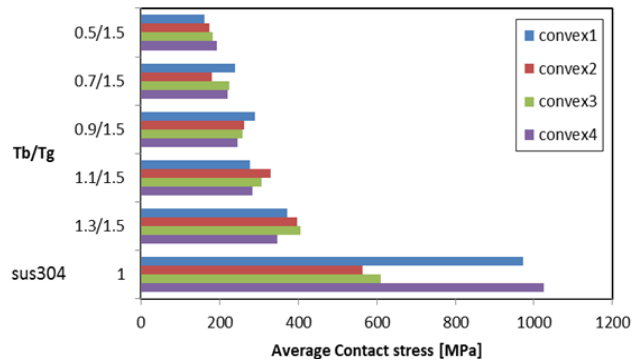


Fig. 21 The average contact stress vs. Tb/Tg for three-layer corrugated metal gasket (400-MPa mode, $E_s/E_b=0.1$, 100kN)

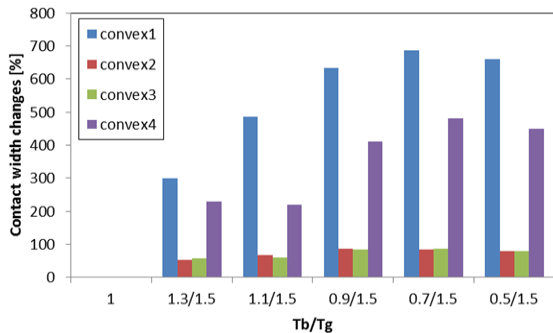


Fig. 22 Percentage contact width increase, gasket 400-MPa mode, axial force 100kN

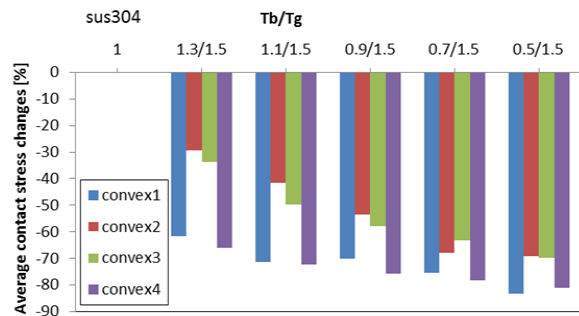
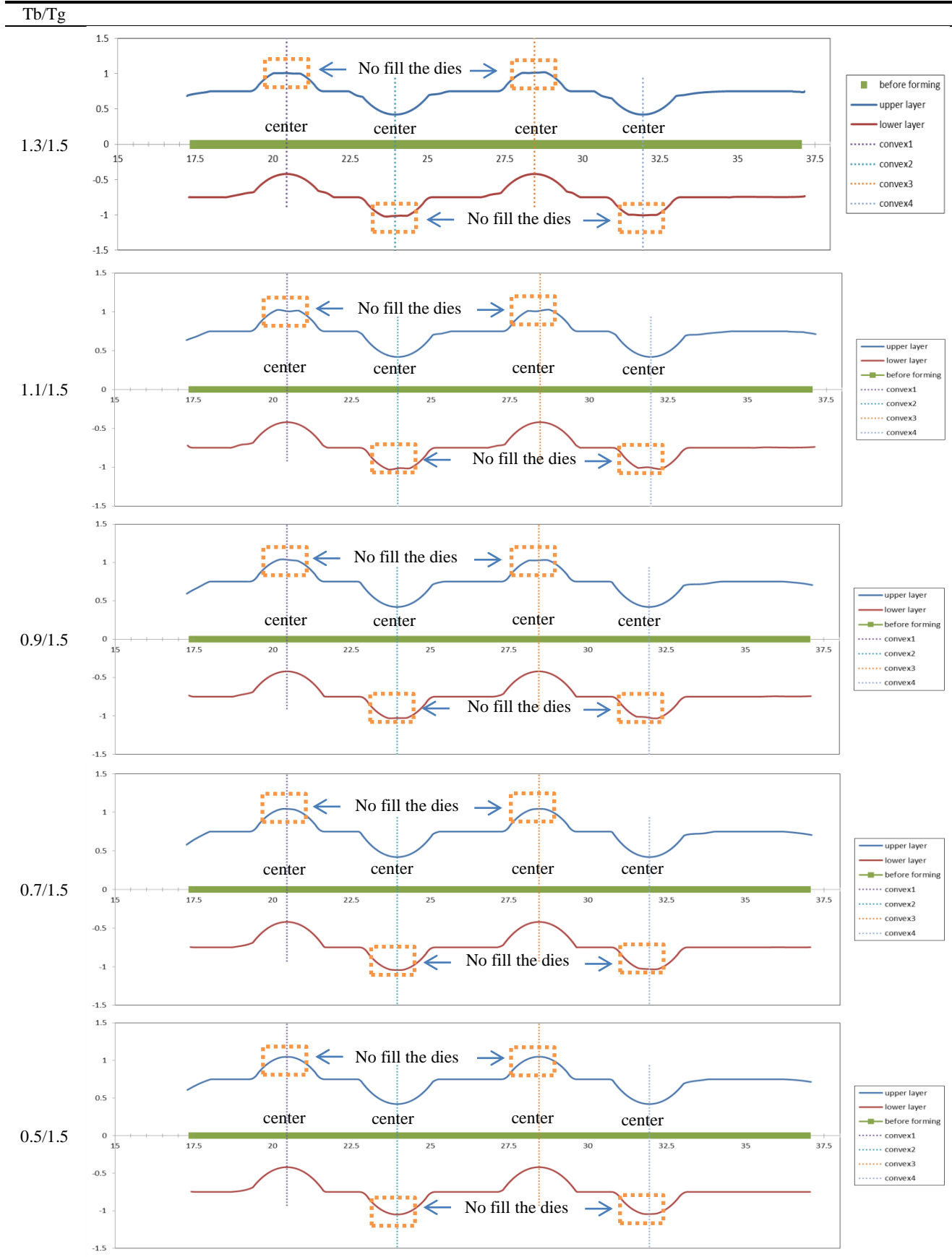


Fig. 23 Percentage average contact stress, gasket 400-MPa mode, axial force 100kN

TABLE IV
 THE DIE FILL DEFECT ON FORMING SIMULATION GASKET THREE-LAYER 400-MPA MODE



ACKNOWLEDGMENT

This project is supported by JSPS KAKENHI Grant Number 26420079 and the Strength of Material Laboratory, Yamaguchi University, Japan. The first author thanks for scholarship support from the Directorate of Higher Education Indonesia cooperated.

REFERENCES

- [1] H.A. Saeed, S. Izumi, S. Sakai, S. Haruyama, M. Nagawa, H. Noda, "Development of New Metallic Gasket and its Optimum Design for Leakage Performance", *Journal of Solid Mechanics and Material Engineering*, Vol. 2, No. 1, 2008, pp. 105-114.
- [2] S. Haruyama, M.A. Choiron, K. Kaminishi, "A Study of Design Standard and Performance Evaluation on New Metallic Gasket", *Proceeding of the 2nd International Symposium on Digital Manufacturing*, Wuhan China, 2009, pp. 107-113.
- [3] M.A. Choiron, S. Haruyama, K. Kaminishi, "Simulation and Experimentation on the Contact Width of New Metal Gasket for Asbestos Substitution", *International Journal of Aerospace and Mechanical Engineering*, Vol. 5, No. 4, 2011, pp. 283-287.
- [4] D. Nurhadiyanto, M.A. Choiron, S. Haruyama, K. Kaminishi, "Optimization of New 25A-size Metal Gasket Design Based on Contact Width Considering Forming and Contact Stress Effect," *International Journal of Mechanical and Aerospace Engineering*, Vol. 6, 2012, pp. 343-347.
- [5] S. Haruyama, D. Nurhadiyanto, M.A. Choiron, K. Kaminishi, "Influence of surface roughness on leakage of new Metal Gasket", *International Journal of Pressure Vessels and Piping*, 111-112, 2013, pp. 146-154.
- [6] S. Haruyama, D. Nurhadiyanto, K. Kaminishi, "Contact Width Analysis of Corrugated Metal Gasket based on Surface Roughness, *Advanced Materials Research*, Vol. 856, 2014, pp. 92-97.
- [7] S. Haruyama, D. Nurhadiyanto, K. Kaminishi, I M.G. Karohika., Mujiono, "Contact Stress and Contact Width Analysis of Corrugated Metal Gasket", *Applied Mechanics and Materials*, Vols. 799-800, 2015, pp. 765-769.
- [8] I. Sakai, H. Ishimaru, G. Horikoshi, 1982, Sealing Concept of Elastic Metal Gasket 'Helicoflex', *Vacuum*, Vol. 32, No. 1, pp. 33-37.
- [9] H. Ishimaru, H. Yoshiki, 1991, Sealing performance of gaskets and flanges against superfluid helium, *Cryogenics*, Vol. 31, June, pp.456-458
- [10] S. Haruyama, I M.G. Karohika, A. Sato, D. Nurhadiyanto, K. Kaminishi, "Development of 25A-Size Three-Layer Metal Gasket by Using FEM Simulation", *International Journal of Mechanical Aerospace, Industrial, Mechatronic and Manufacturing Engineering*, Vol:10, No:3, 2016, pp.555-561.
- [11] J.K. Kim, T.X. Yu, 1997, Forming and failure behavior of coated, laminated and sandwiched sheet metal: a review, *Journal of Materials Processing Technology* 63, pp.33-42.